NASA

Technical Memorandum **79633**

Early Results from ISEE-A Electric Field Measurements

J. P. Heppner
N. C. Maynard
T. L. Aggson

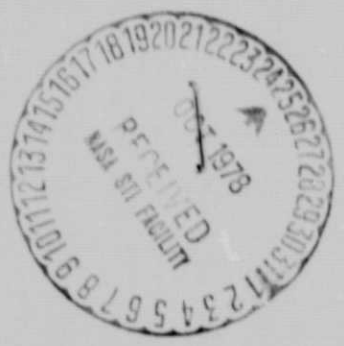

JUNE 1978

National Aeronautics and
Space Administration

Goddard Space Flight Center
Greenbelt, Maryland 20771

ABSTRACT

The double probe, floating potential instrumentation on ISEE-A is producing reliable direct measurements of the ambient DC electric field at the bow shock, at the magnetopause, and throughout the magnetosheath, tail plasma sheet and plasmasphere. In the solar wind and in middle latitude regions of the magnetosphere spacecraft sheath fields obscure the ambient field under low plasma flux conditions such that valid measurements are confined to periods of moderately intense flux. Initial results show: (a) that the DC electric field is enhanced by roughly a factor of two in a narrow region at the front, increasing $\underline{B}$, edge of the bow shock, (b) that scale lengths for large changes in $\underline{E}$ at the sub-solar magnetopause are considerably shorter than scale lengths associated with the magnetic structure of the magnetopause, and (c) that the transverse distribution of $\underline{B}$-aligned $\underline{E}$-fields between the outer magnetosphere and ionospheric levels must be highly complex to account for the random turbulent appearance of the magnetospheric fields and the lack of corresponding time-space variations at ionospheric levels. Spike-like, non-oscillatory, fields lasting < 0.2 seconds are occasionally seen at the bow shock and at the magnetopause and also intermittently appear in magnetosheath and plasma sheet regions under highly variable field conditions. These suggest the existence of field phenomena occurring over dimensions comparable to the probe separation and $\leq c/\omega_{pe}$ (the "characteristic" electron cyclotron radius) where ω_{pe} is the electron plasma frequency.

Introduction

The symmetric double probe, floating potential technique for measuring DC and low frequency electric fields which was initially described in a 1964 proposal (Aggson and Heppner, 1964) has since been employed on a number of rockets and satellites. In dense plasmas (e.g., >100 el./cm^3) the technique has been highly successful with relatively modest probe separations. In weak plasmas (e.g., <10 el./cm^3) results from OGO, IMP, S^3, and Hawkeye satellites have shown that acquisition of valid measurements of the ambient DC field is a sensitive function of the probe separation and the ambient plasma flux and that each increase in the probe separation has extended the space-time applicability of the technique (see e.g., Aggson and Heppner, 1977; Heppner et al., 1978). Thus with the substantial increase in probe separation on ISEE-A (see Figure 1) it was anticipated that valid measurements would be obtained over more extensive spatial regions and for greater periods of time in regions of marginal plasma flux. Preliminary scans of data taken in various plasma regimes confirm this anticipation.

The following statements briefly characterize the status of the measurements.

(1) At the bow shock, at the magnetopause, throughout the magnetosheath, and near and inside the plasmapause, the measurements examined to date have been valid and accurate.

(2) In the solar wind and in middle latitude regions of the outer magnetosphere, the measurements during periods of low activity are most commonly dominated by strong solar oriented sheath fields associated with the spacecraft and its conducting appendages. Valid measurements are obtained under moderately disturbed conditions when the plasma density increases.

(3) From smaller samplings of data in the geomagnetic tail it appears that measurements in the plasma sheet will be valid most of the time.

(4) Data taken under eclipse conditions in the near earth tail are free of sheath effects and thus demonstrate the photoelectron character of the sheath in sunlight in low density plasmas. From eclipse data it is apparent that DC fields as weak as 20 μ volts/meter can be accurately measured. This accuracy also appears evident, but is less definitively proven, in the magnetosheath when the component in the spin plane is small.

(5) Considerable attention has been directed toward examining the signal behavior when the electron gun is active and/or currents are drawn by the spheres or shields of the electric field probes (F. Mozer experiment) extended perpendicular to our (Figure 1) double probe axis. What one wants to know is whether or not these bias functions, which drive the spacecraft positive relative to the probes, will favorably alter the sheath parameters. In all cases and modes examined the bias functions have introduced effects which clearly do not lead to the measurement of ambient fields with the Figure 1 probes. The effects involve both large amplitude sheath voltages and asymmetries and these obliterate any possibility of obtaining valid measurements in weak plasmas when the bias functions are operative.

(6) High voltage spacecraft charging events have not been encountered in the data examined sunward from the earth. Several charging events have been detected in near tail regions but their statistical prevalence and coincidence with geophysical events has not been evaluated.

The present paper is oriented toward illustrating typical electric field measurements in raw data form. This illustrates that the floating potential measurements are direct measurements, without correction or

manipulation. The only computation for the instantaneous electric field in the spin plane (E_{xy}) is the division by $\underline{d}$, the probe separation shown in Figure 1. The "Common Mode" voltage, V_a-V_s, is a highly useful diagnostic of plasma conditions surrounding the spacecraft. It is also sampled frequently using the same 14 bit A/D converter that gives the differential voltage, V_a-V_b. At low bit rates, V_a-V_b and V_a-V_s are sampled 24 and 12 times per spin cycle, respectively.

Additional experiment outputs include: a number of sub-commutated measurements at selected angles indexed to the sun and the magnetic field directions, measurements of AC fields in 8 filter channels between 0.19 and 1900 Hz, and measurements of the plasma impedence. These functions and the various options, such as blanking-out or leaving-in the sun pulse that occurs in weak plasmas when the probes are aligned with the sun, are described in Heppner et al. (1978).

Presentation in the form of raw data also enables one: (a) to illustrate invalid data (see discussions related to Figures 2, 3, and 6), and (b) to illustrate the existence and prevalence of short duration (e.g., 0.1 to 0.2 second) spikes and the sharpness of electric field changes. These latter features, which will be more completely studied using high bit rate data in the future, are of particular interest in that they suggest short-lived or small scale electrostatic departures from the hydromagnetic $\underline{E} + \underline{v} \times \underline{B} = 0$, relationship.

In general, whether examining shock, magnetopause, magnetosheath, or plasma sheet data the short period or small scale variability of the measured (i.e., as opposed to "model") electric field is its most evident characteristic. Thus, raw data presentation is appropriate from this standpoint as well as those noted above. It is envisaged that various modes of time-space data averaging will have to be tried to arrive at the most meaningful representations of large scale distributions. Particularly within the magnetosphere finding an averaging

process that yields the large scale features evident at ionospheric levels represents a major challenge. In turn this implies that many of the small scale magnetospheric field structures, or equivalent time variations, do not directly map along equipotential magnetic field lines to high latitude ionospheric levels.

Coordinates and Solar Wind Measurements

Figure 2 is a sample of the field E_{xy} in the spin plane in the solar wind at a time when the ambient field magnitude was variable. It also serves to illustrate the coordinates. $\phi=0^{o}$ marks the time when the a probe is pointing at the sun which is also the direction of the x axis in solar-ecliptic coordinates. As shown the maximum + E_{xy} field is directed toward $\phi=90^{o}$ which is also the y axis in solar-ecliptic coordinates. Subject to the assumption that the bulk velocity, v, of the solar wind is radially away from the sun, the validity of the field measured is evident from the fact that the ambient field is oriented normal to v. The signal distortion, or spike, which occurs at $\phi=0^{o}$ and $\phi=180^{o}$ is a consequence of the sudden decrease in photoemission from the probes when they align with the sun. This example illustrates changes in the appearance of the $\phi=0^{o}$ and 180^{o} sun pulse under variable conditions in the ambient plasma, and also that the measurements near $\phi=90^{o}$ and 270^{o} are not affected by either the pulses or the spacecraft sheath.

In contrast to the valid ambient field measurements in Figure 2, invalid measurements appear in the solar wind in Figure 3 in the regions labeled SW. In these cases one notes that the signal maximum occurs coincident with the sun aligned pulse-like distortions at $\phi=0^{o}$. The electric field that is measured in these cases is simply a sun-aligned field stemming from the spacecraft. In the presence of extremely low densities in some regions of the magnetosphere the rather broad pulses at $\phi=0^{o}$ and 180^{o} in Figure 3 become much narrower and it becomes more appropriate to call them "sun pulses" or "sun spikes". The pulses

located at peak and trough values of the sheath field evident between 22:59:04 and 22:59:10 in Figure 6 roughly illustrate this characteristic.

Bow Shock Fields

The three shock encounters, all within one minute, shown in Figure 3 illustrate the abruptness of the electric field change at the shock. This abruptness must also be present in the plasma flux to produce the transition from sheath measurements in the solar wind to ambient field measurements at the shock and on the magnetosheath side of the shock. In the first example (top trace) the transition occurs within a fraction of a second, between 19:29:33 and 19:29:34 and coincides with the spike response having twice the magnitude of the adjacent magnetosheath field. In the next encounter (middle trace) a small spike again appears. The third (bottom) trace suggest a less abrupt transition without a spike field; however, it must be kept in mind that for a feature lasting only a fraction of a second the probes can, at that instant, be in an orientation transverse to the field and thus miss its occurrence.

Relative to the many past studies of the magnetic field structure in the bow shock it is desirable to know the relative location of the abrupt electric field transition and the associated small (i.e., roughly a factor of two) enhancement in the electric field magnitude which is frequently, but not always, present at the shock. Figure 4 provides an example relative to the magnetic field. In this case the transition from sheath field to ambient field measurements, near 13:22:23 is separated about two seconds from the largest spike at 13:22:25 and there is a total period of about 5 seconds (to 13:22:30) when the average field is more intense than at subsequent times. When related to the magnetic field structure it is apparent that the enhanced DC E-field is coincident with the leading edge and with increasing $\underline{B}$ at the shock front. Moving further into this shock, which has a magnetic profile very much like the model shock presented by Heppner et al. (1967), the enhanced $\underline{B}$ section

which lasts about 30 seconds coincides with a region of highly irregular electric fields with amplitudes of several volts/Km. As shown this is evident in the 6-19 Hz band as well as in the d.c. measurements.

From observations in the VLF band it has previously been argued (Fredricks et al., 1970): (a) that the scale length for electrostatic turbulence in the bow shock is defined by c/ω_{pe}, the "electron inertial length" or "characteristic electron cyclotron radius" where ω_{pe} is the electron plasma frequency, and (b) that the bow shock electrostatic turbulence is associated in time with regions of steep slope in (B). These arguments appear to also fit the DC observations and in fact appear to be even more definitive at DC and low frequencies in placing the peak DC field at the leading edge of the shock.

Magnetosheath Fields

As anticipated from the well known variability of plasmas and magnetic fields in the magnetosheath, and from previous Imp-6 and 8 electric field measurements, an endless variety of electric field behaviors is encountered. Figure 5 provides several examples from a single magnetosheath crossing. The measurements in this region are free of sheath effects and one does not see the sun pulses that were apparent in the solar wind. This particular pass near 11 hours local time was chosen for illustration to provide continuity with Figure 6 and to show an interval of exceptional strong fields. The strong field (bottom trace) occurred about 7 minutes after an interval when the spacecraft was inside the magnetosphere for several minutes. Between the magnetopause crossing preceding the Figure 5 bottom trace and the next magnetopause crossing there was an interval of about 75 minutes. Thus the strong field occurred after the magnetopause had moved much closer to the earth. When compared with data from the on-board electron spectrometer (Ogilvie experiment) it was found that the occurrence of this strong field (12 volts/Km) coincides exactly with a brief interval when the

bulk flow jumped to 450 Km/sec with essentially no change in plasma density.

Magnetopause Fields

The magnetopause crossing shown in Figure 6 near 22:58:55 is one of several that occurred more than an hour after the last Figure 5 example. This particular crossing is presented because it shows the strongest electric field observed near the sub-solar point. As shown, the field reached a magnitude of 23 volts/Km for about 0.1 seconds when the probes were at a ϕ angle of 118^{o}. This, of course, does not reveal the maximum field during this 0.1 second interval as it would be fortuitous for the antenna-probe orientation to be parallel to the total electric field vector. Similar spikes of lesser magnitude also appear in this crossing at other angles; all, however, point away from the sun. In total, these imply the existence of sharp transients or, alternatively, narrow (e.g., 0.1 to 1.0 Km) strong field shells or filaments.

Other interesting aspects of the Figure 6 example are: (a) the apparent stagnation in the magnetosheath between 22:58:34 and 22:58:50 (i.e., a 16 sec. interval), (b) the total duration of strong (E) between roughly 22:58:54 and 22:59:02 (i.e., an interval of <8 seconds), and (c) the abrupt transition to low plasma flux and spacecraft sheath fields between 22:59:01 and 22:59:03 (i.e., an interval of <2 seconds). Prior to the study of numerous crossings and examination of the simultaneous plasma and magnetic field signatures detailed interpretation would be premature. It does, however, appear clear from this example and others that near the sub-solar nose of the magnetosphere scale lengths for large changes in the electric field are considerably less than the scale lengths associated with the magnetic field structure of the magnetopause. In terms of the classical pictures of the microstructure of the magnetopause (e.g., see review by Willis, 1975) this implies an association between strong DC E-fields and the electron penetration, c/ω_{pe}, as

opposed to associations with dimensions as large as the ion cyclotron radius. In viewing the large amplitude spikes of <0.2 seconds duration one must, however, keep two reservations in mind: (a) these features could be a unique form of time transient at the boundary that is not correctly interpreted in terms of spatial scale, and (b) if these spikes represent a spatial structure it is also possible that they are dimensionally thinner than c/ω_{pe}. These reservations may also be applicable to the spikes observed at the bow shock.

Mid-Night, Near-Tail Fields

In advance of routine tape processing, strip chart records were taken in real time on a number of passes in the midnight sector to examine signal characteristics while passing into and out of solar eclipse. The details which reveal the photoelectron character of the sheath will be presented elsewhere. The item of immediate interest is that measurements on some passes showed a greater diversity of ambient field behaviors than one would expect from extrapolation of previous low altitude (e.g., <2000 Km) observations in the midnight auroral belt. Figure 7 provides a "quiet" field reference near the magnetic equator. In this case the field was relatively stable and weak with $E_{xy} \doteq 0.1$ to 0.15 volts/Km but may have gradually changed direction as indicated by the phase relative to the $\phi=0^{o}$ direction (Note: because the solar direction, $\phi=0^{o}$, is extrapolated from sunlit regions the phase angle could be in error). The small fluctuations of 0.01 to 0.02 volts/Km superimposed on the spin signal are believed to be ambient field fluctuations. In total there is no reason to suspect that extrapolation of this field to ionospheric levels would conflict with an assumption of equipotential mapping along magnetic field lines.

Figure 8, in contrast to Figure 7, shows a diversity of field behaviors, all occurring within several minutes of time, during eclipse near a magnetic latitude of 22^{o}. Taking into account reasonable values for the convergence of the flux tube at ionospheric levels the magnitudes,

ranging from 0.1 to 4.0 volts/Km, are not out of line with magnitudes that might be present at ionospheric levels. However, in terms of existing observations an ionospheric counterpart for the "turbulent" or random appearance of this magnetospheric field is highly unlikely. From the scanning of data taken in the tail plasma sheet it is also apparent that the Figure 8 example is not unique in that similar randomness appears frequently. This diversity of field behavior is also somewhat analogous to the frequent changes in field behavior encountered in the magnetosheath.

At this writing, dominant or characteristic time and/or space scale factors for these field changes have not been identified. The middle trace of Figure 8, for example, is dominated by spatial scale factors comparable to the probe dimensions as indicated both by the lack of maximum amplitude at the spin period (3 seconds) and the existence of several spike type field changes. Rotations of the dominant DC field at rates comparable to the spin period are also present (top trace between 16:19:20 and 16:19:23) in the presence of strong fields. In total it appears safe to say that large field changes can be found over any time scale one chooses. Thus analysis techniques that will reveal the outer magnetosphere counterpart of the comparatively orderly patterns of the global ionospheric electric field are not presently apparent. This also implies that between the outer magnetosphere and the ionosphere the distribution of B-parallel components of the electric field, as viewed through surfaces transverse to $\underline{B}$, must be highly complex.

References

Aggson, T. L. and J. P. Heppner: 1964, A Proposal for Electric Field Measurements on ATS-1, NASA/GSFC (preprint July 1964).

Aggson, T. L. and J. P. Heppner: 1977, J. Geophys. Res., 82, 5155.

Fredricks, R. W., G. M. Crook, C. F. Kennel, I. M. Green, F. L. Scarf, P. J. Coleman, and C. T. Russell: 1970, J. Geophys. Res., 75, 3751.

Heppner, J. P., E. A. Bielecki, T. L. Aggson, and N. C. Maynard: 1978, Geoscience Electronics (in press).

Heppner, J. P., M. Sugiura, T. L. Skillman, B. G. Ledley, and M. Campbell: 1967, J. Geophys. Res., 72, 5417.

Willis, D. M.: 1975, Geophys. J. R. Astr. Soc., 41, 355.

Figure Captions

Figure 1: Double probe, wire antenna dimensions and measured DC parameters.

Figure 2: Measurements of a variable field in the solar wind (raw data).

Figure 3: Sequence of bow shock crossings at locations labeled (S). (M) designates magnetosheath. Measurements in the solar wind (SW) are dominated by the spacecraft sheath.

Figure 4: Bow shock crossing (see text).

Figure 5: Sampling of field variations in the magnetosheath.

Figure 6: Example of strong fields at the magnetopause (22:58:54 to 22:59:02) (see text).

Figure 7: Samples of a weak field in the midnight magnetosphere.

Figure 8: Samples illustrating a diversity of field behaviors in the midnight magnetosphere.

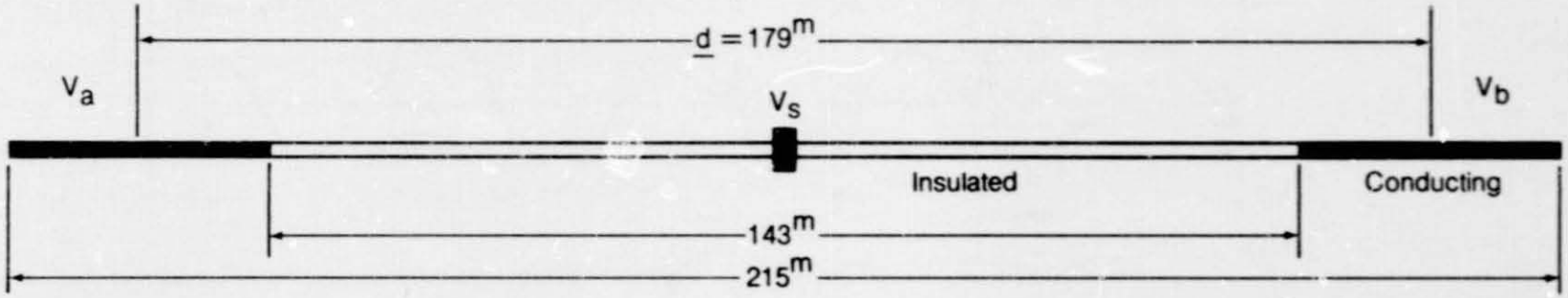

"COMMON MODE" VOLTAGE = $V_a - V_s$

DIFFERENTIAL VOLTAGE = $V_a - V_b$

ELECTRIC FIELD = $E_{xy} = (V_a - V_b)/d$

FIGURE 1

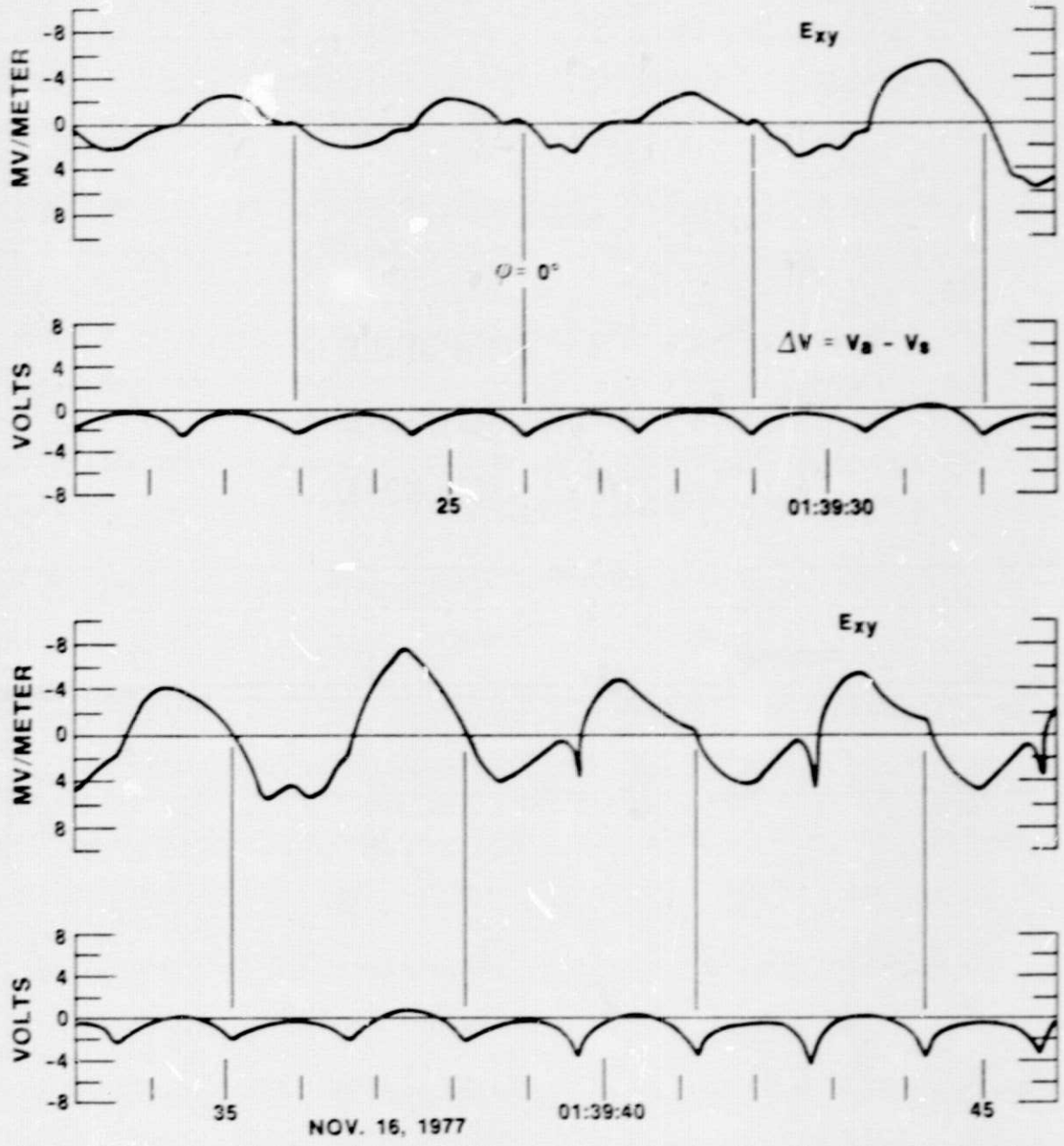
MV/METER
-8
-4
0
4
8
E_{xy}
$\varphi = 0°$
VOLTS
8
4
0
-4
-8
$\Delta V = V_a - V_s$
25
01:39:30
MV/METER
E_{xy}
VOLTS
35
NOV. 16, 1977
01:39:40
45

FIGURE 2

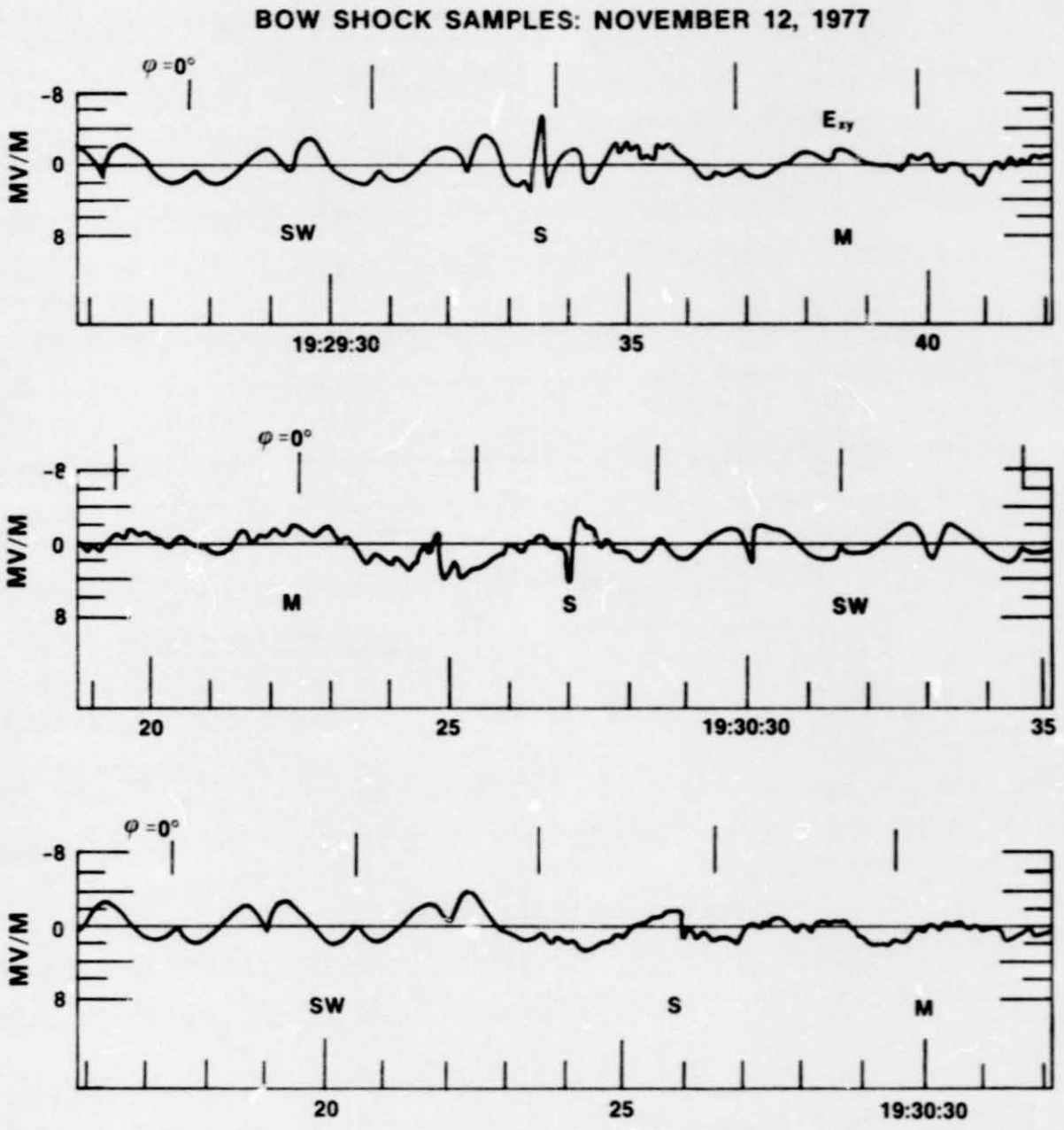

FIGURE 3

ISEE-1 BOW SHOCK CROSSING

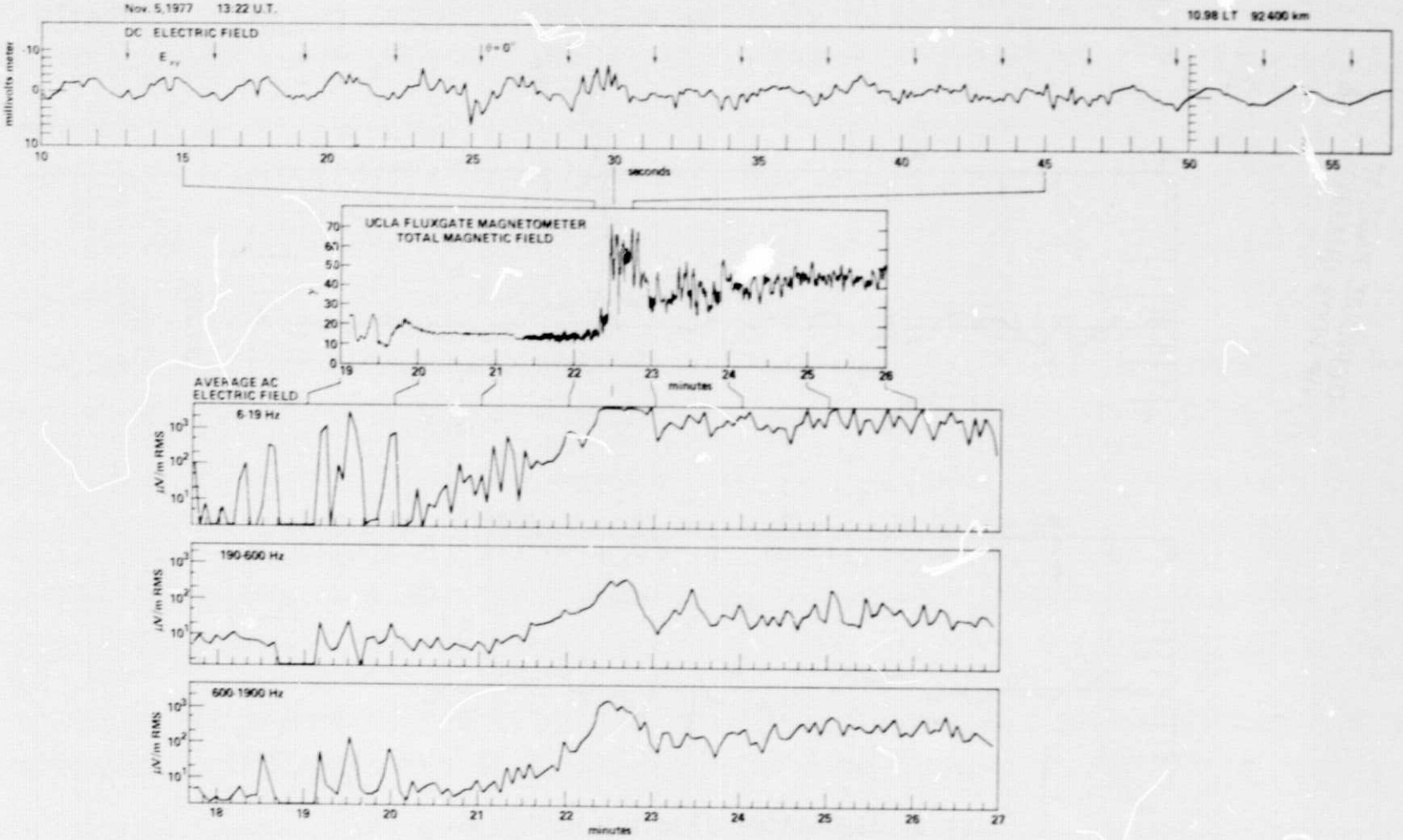

FIGURE 4

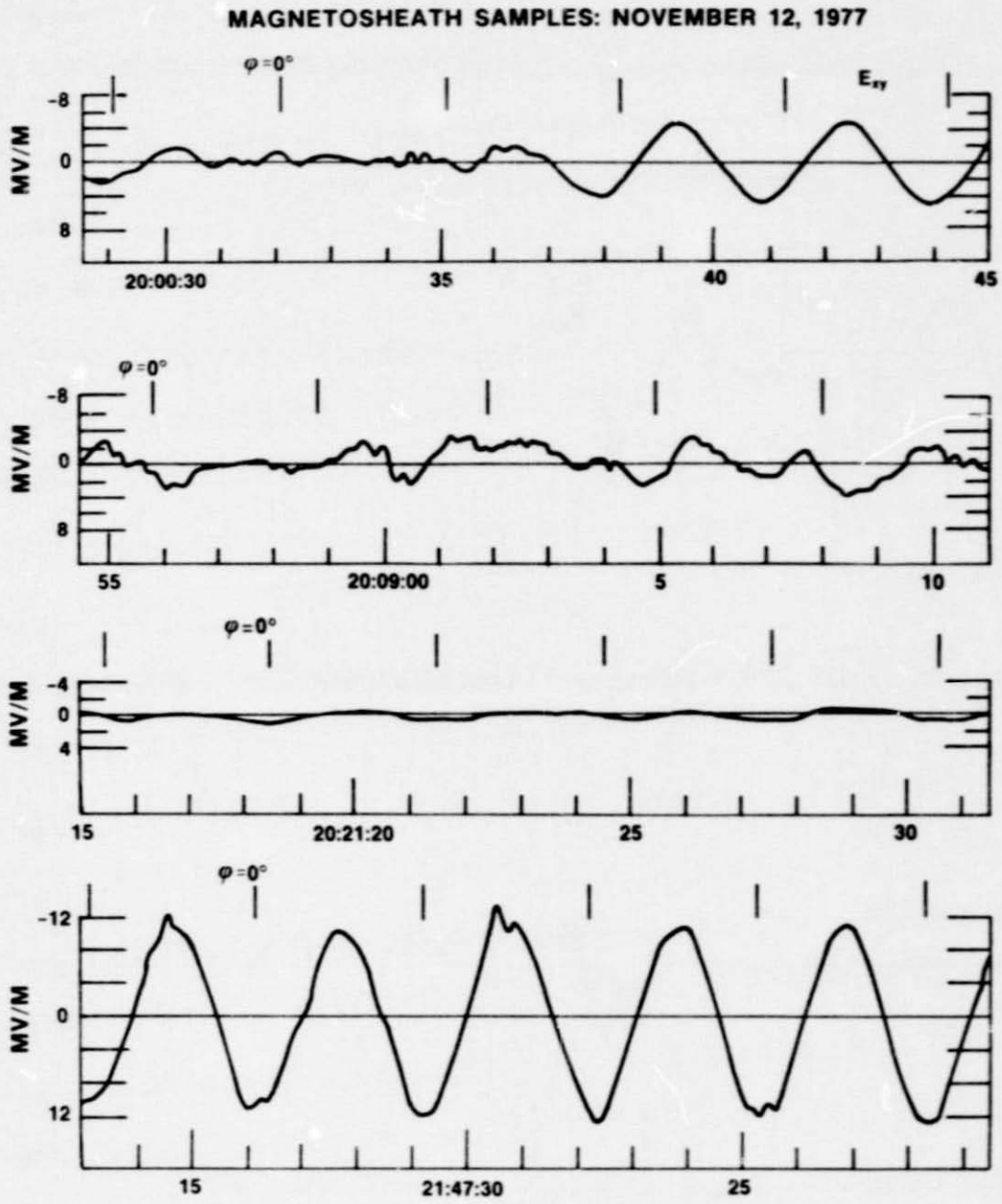

FIGURE 5

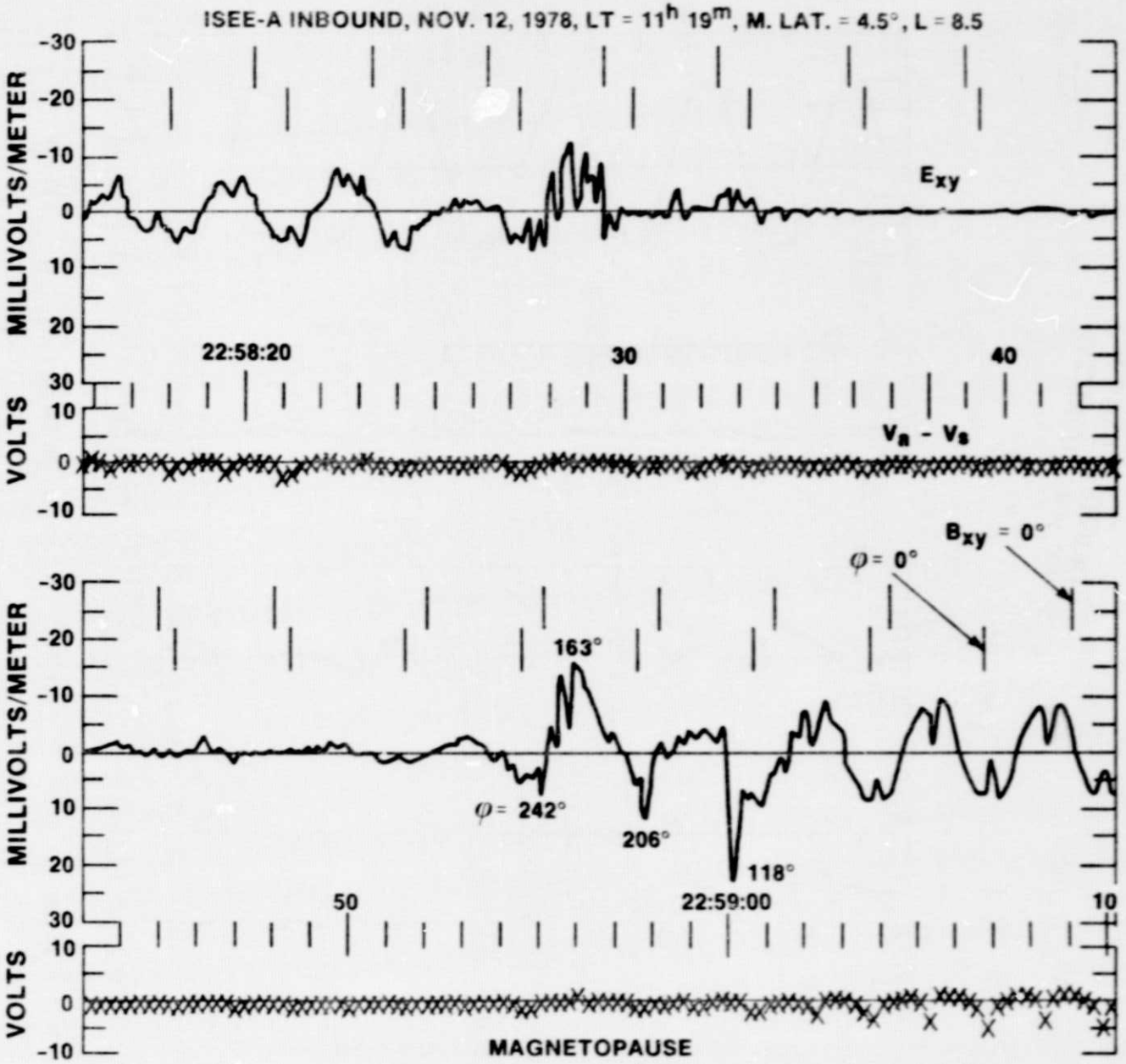
ISEE-A INBOUND, NOV. 12, 1978, LT = 11h 19m, M. LAT. = 4.5°, L = 8.5
MILLIVOLTS/METER
-30
-20
-10
0
10
20
30
E_{xy}
22:58:20
30
40
VOLTS
30
10
0
-10
$V_a - V_s$
B_{xy} = 0°
φ = 0°
MILLIVOLTS/METER
163°
φ = 242°
206°
118°
50
22:59:00
10
VOLTS
MAGNETOPAUSE

FIGURE 6

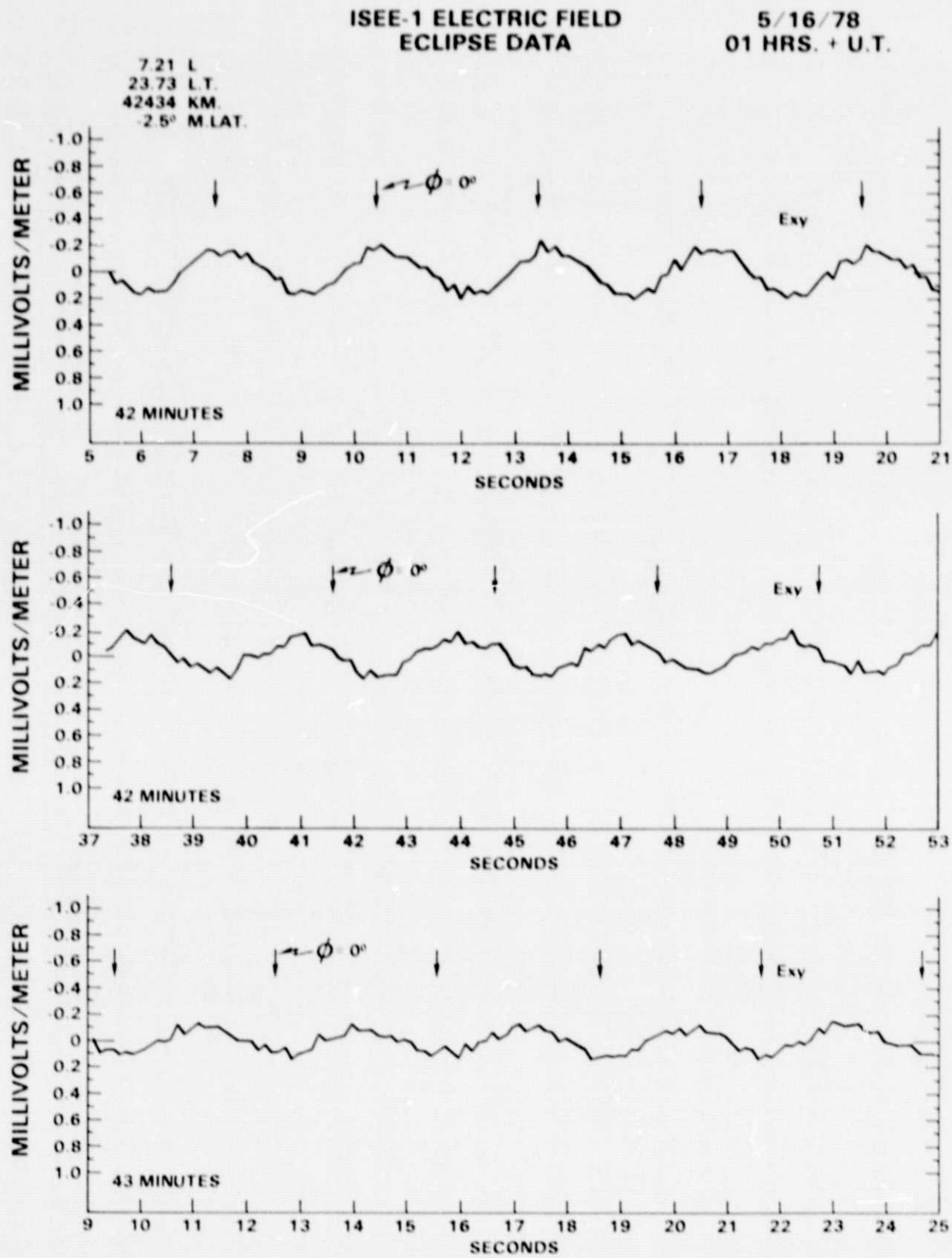

FIGURE 7

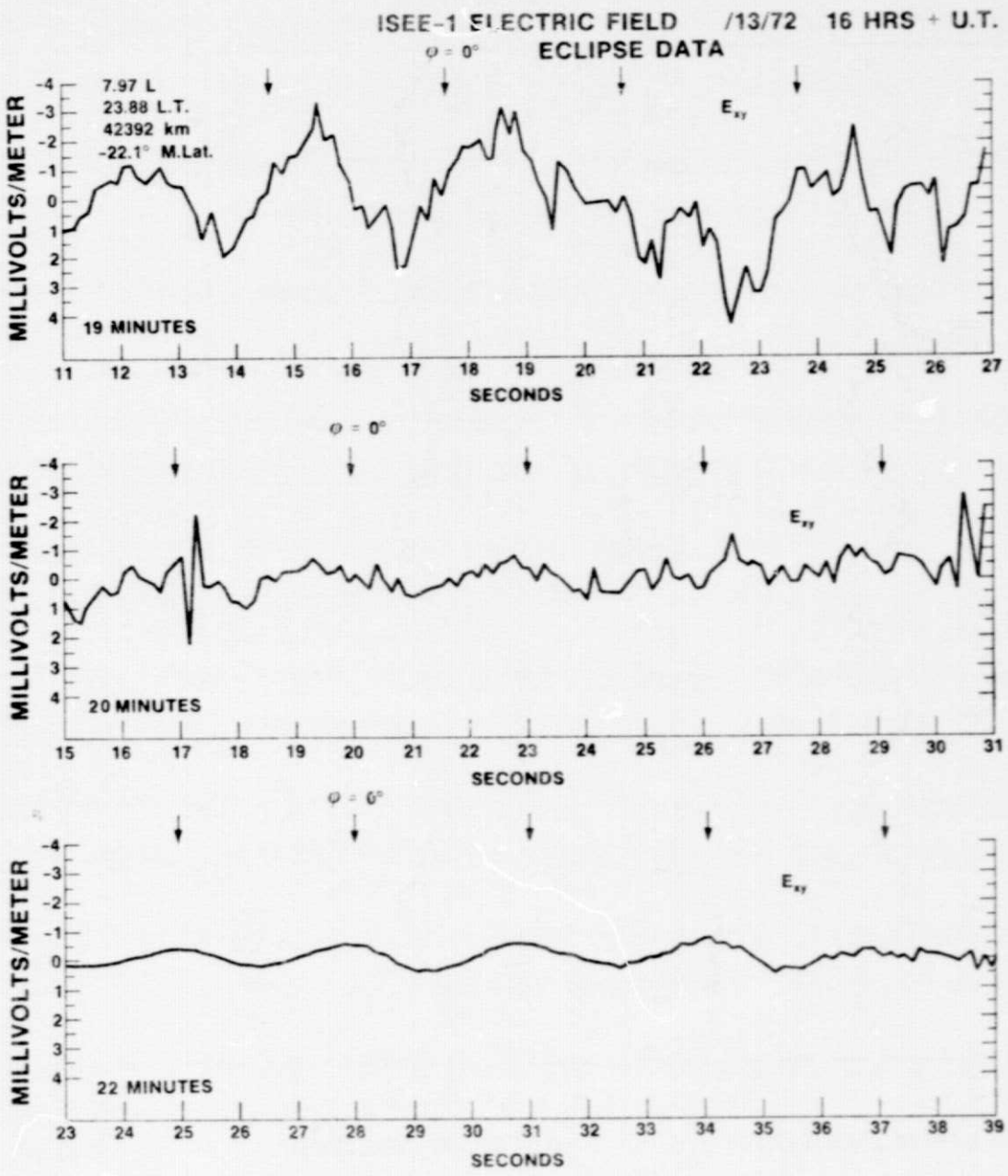
ISEE-1 ELECTRIC FIELD /13/72 16 HRS + U.T.
ECLIPSE DATA
φ = 0°
7.97 L
23.88 L.T.
42392 km
-22.1° M.Lat.
E_xy
MILLIVOLTS/METER
19 MINUTES
SECONDS
φ = 0°
E_xy
MILLIVOLTS/METER
20 MINUTES
SECONDS
φ = 0°
E_xy
MILLIVOLTS/METER
22 MINUTES
SECONDS

FIGURE 8